Journal of Materials Chemistry A

PAPER

View Article Online
View Journal | View Issue

Cite this: J. Mater. Chem. A, 2015, 3, 6187

Cyclodextrin modified microgels as "nanoreactor" for the generation of Au nanoparticles with enhanced catalytic activity†

He Jia,[a] Dominik Schmitz,[b] Andreas Ott,[a] Andrij Pich*[b] and Yan Lu*[a]

Received 9th January 2015
Accepted 13th February 2015

DOI: 10.1039/c5ta00197h

www.rsc.org/MaterialsA

We report a facile and green method for the fabrication of hybrid microgels by the immobilization of catalytically active Au nanoparticles in α-cyclodextrin (α-CD) modified poly(*N*-vinylcaprolactam) (PVCL) microgels without addition of reducing agent and surfactant. It has been shown that only in the case of α-CD modified microgels metal particles were immobilized inside the colloidal gels, which is due to a coordination of the cyclodextrin molecules to the surface of Au nanoparticles. The PVCL-α-CD-Au composite particles can work efficiently as catalyst for the reduction of aromatic nitro-compounds by using the reduction of 4-nitrophenol (Nip) and 2,6-dimethyl-4-nitrophenol (DMNip) as model reactions. Most importantly, due to the selective binding ability of α-CDs to certain reagents, the synthesized hybrid microgels show different catalytic activity for the target compounds during the catalytic reactions: a significant enhancement in the catalytic activity has been observed for the reduction of Nip, while no obvious effect has been found for the reduction of DMNip.

Introduction

Stimuli-responsive microgels have gained increasing attention in recent years as they can undergo reversible conformational changes in response to external stimuli, which are often accompanied by variations in the physical and chemical properties of the polymers, such as volume, shape, surface area, solubility, or mechanical properties.[1–4] More importantly, the networks of the microgels are well-suited for *in situ* synthesis of catalytically active metal nanoparticles. Because of the availability of free spaces in the swollen gel networks, the stimuli-responsive microgels can provide excellent nucleation and growth environments for nanoparticles without aggregation.[5–8] Thus, different microgel systems have been developed and applied as "nanoreactors" for the deposition of metal nanoparticles (NPs).[9–12] Among them, poly(*N*-isopropyl acrylamide) (PNIPAM) and poly(*N*-vinylcaprolactam) (PVCL) are the most commonly used temperature responsive microgels.[13–16] For example, Liz-Marzán *et al.* have successfully combined NIPAM polymerization on the surface of highly magnetic iron oxide nanocrystals and *in situ* nucleation and growth of Ag nanoparticles.[17] They also found that the temperature-responsive PNIPAM shell with limited cross-linking allowed for particularly efficient control of the catalysis of the embedded Au nanoparticles.[18] Kumacheva *et al.* used polyampholyte poly(*N*-isopropyl acrylamide-*co*-acrylic acid-*co*-vinyl imidazole) (poly(NIPAm-AA-VI)) microgels as carriers to synthesize Au nanorods within the microgels.[19] Recently Suzuki *et al.* have synthesized thermosensitive microgels by using NIPAM and 3-(methacrylamino) propyltrimethylammonium chloride (MAPTAC) as the monomers to immobilize Au nanoparticles. In their study, the cationic sites in the microgels were used to nucleate particle growth, while $NaBH_4$ and dimethylamineborane were used as the reducing agent.[20] In our previous study, thermosensitive polystyrene (PS)–PNIPAM core–shell microgels have been applied to immobilize Ag nanoparticles as well as Au, Rh, Pt nanoparticles.[21,22] Besides of PNIPAM microgel particles, PVCL microgels have been also applied as carriers for inorganic nanoparticles. For example, poly[(*N*-vinylcaprolactam)-*co*-(acetoacetoxyethyl methacrylate)] (PVCL/AAEM) microgels have been developed as carriers for the deposition of ZnS nanoparticles by reaction of zinc acetate and thioacetamide under ultrasonic agitation.[23]

In most of these studies, the synthesis of metal nanoparticles using microgels as template has been always conducted in the presence of strong reducing agents, such as $NaBH_4$, H_2, NH_2NH_2 and so forth.[24–29] The use of strong reducing agents will

[a]*Soft Matter and Functionmal Materials, Helmholtz-Zentrum Berlin für Materialien und Energie, Hahn-Meitner-Platz 1, 14109 Berlin, Germany. E-mail: yan.lu@helmholtz-berlin.de*

[b]*Functional and Interactive Polymers, Institute of Technical and Macromolecular Chemistry, RWTH Aachen University, DWI Leibniz Institute for Interactive Materials, Forckenbeckstr. 50, D-52056 Aachen, Germany. E-mail: pich@dwi.rwth-aachen.de*

† Electronic supplementary information (ESI) available: The amount of α-CD and the size changing of the microgels were measured by FTIR and DLS; the color changing and the stability of the microgels loaded with and without Au were measured by UV-vis and LUMiSizer; the complexation between Nip and microgels, the catalytic process of DMNip were measured by UV-vis; the size and complexation with Nip of CTAB-Au were measured by TEM and UV-vis. See DOI: 10.1039/c5ta00197h

limit the types of microgels according to the functionalities within the polymer with respect to chemical stability. Moreover, such approaches provide hybrid structures with a random distribution of metal nanoparticles inside the microgel structure. Some polymers, such as poly(*N*-vinyl-2-pyrrolidone) and polyvinylpyrrolidone (PVP), can work both as the reducing agents and the surfactants for the preparation of homogeneous metal nanoparticles.[30,31] However these polymers could not work as the "nanoreactors" as observed for microgels. More recently, we have reported that a newly developed *N*-vinylcaprolactam/acetoacetoxyethyl methacrylate/acrylic acid based microgel displays *in situ* reductive reactivity towards $HAuCl_4$, forming hybrid polymer–Au nanostructures at ambient temperature without additional reducing agents.[32] However, it is still a big challenge to develop an active "nanoreactor" based on microgel particles for the generation of catalytic active metal nanoparticles containing specific/selective binding domains on the surface without the use of reducing agents and surfactant/ligands. This will open new possibilities for the synthesis of metal hybrid colloidal particles directly under mild aqueous conditions and facilitate the use for catalytic applications.

In this paper, poly(*N*-vinylcaprolactam) (PVCL) microgel modified with reactive α-cyclodextrins (α-CDs) has been synthesized and successfully used to reduce and stabilize Au nanoparticles *in situ* without any additional surfactant and reducing agents. The incorporation of CD molecules into the microgel leads to a novel "nanoreactor" for metal nanoparticles: first of all, both PVCL and CDs can work as the reducing agents in the generation of Au nanoparticles.[33] Secondly, the CD molecules can serve as a stabilizer for the Au nanoparticles by chemisorption to the nanoparticle surface through the hydroxyl groups.[34] The size of Au nanoparticles generated in the microgels can be controlled. Thus, no additional surfactant/capping agents are required for the synthesis, which will efficiently reduce the influence of surfactants on the surface properties and catalytic activity of Au nanoparticles. Most importantly, because of the different complexation abilities of CDs with aromatic nitro compounds with various structures,[35] the Au nanoparticles could show specific/selective binding abilities to certain reagents resulting in enhanced catalytic activity. We will demonstrate this by comparing the catalytic reduction of 4-nitrophenol (Nip) and 2,6-dimethyl-4-nitrophenol (DMNip) in the presence of PVCL-α-CD-Au nanoparticles. The present approach provides a novel and "green" route for the fabrication of Au nanoparticles embedded in α-CD modified microgel "nanoreactors", which will extend the controlled synthesis of catalytically active metal nanoparticles with specific surface properties.

Experimental section

Materials

Gold(III) chloride trihydrate ($HAuCl_4 \cdot 3H_2O$), sodium hydroxide (NaOH), sodium borohydride ($NaBH_4$), solid cetyltrimethylammonium bromide (CTAB), ascorbic acid (AA), acetoacetoxyethyl methacrylate (AAEM), *N*-vinylcaprolactam (VCL), *N*,*N*′-methylene-bis-acrylamide (BIS), 2,2′-azobis(2-methylpropionamidin) dihydrochloride (AMPA), trisodium citrate, 2,6-dimethyl-4-nitrophenol (DMNip) and 4-nitrophenol (Nip) were supplied by Aldrich. VCL was purified by distillation *in vacuo*. All other reactants were used without further purification. Water was purified by a Milli-Q system.

Synthesis of PVCL-α-CD microgel

The synthesis of the aqueous microgel dispersion was done using precipitation polymerization according to the literature.[36] Acrylate modified α-cyclodextrin with an average substitution degree of three was prepared according to the literature[37,38] and used for the synthesis of CD-modified microgels. The monomers, 2.06 g (14.72 mmol) VCL, 0.05 g AAEM (0.23 mmol), 0.02 g BIS (0.13 mmol) and 0.05 g (0.04 mmol) or 0.30 g (0.26 mmol) α-CD acrylate, respectively, were dissolved in 147 ml of water and added to a double-wall glass reactor with KPG-stirrer. The reaction mixture was purged with nitrogen at 70 °C under stirring (200 rpm). Afterwards 0.02 g (0.07 mmol) AMPA in 3 ml degased water was added. After some minutes, a turbid dispersion was formed and the reaction was carried out for 8 h. Obtained microgels were purified by dialysis using cellulose membranes with a MWCO of 12 000–14 000 Da. The dialysis was carried out for three days. To determine the actual α-CD content, a freeze-dried sample was analyzed by FTIR-spectroscopy.

Synthesis of PVCL-α-CD-Au microgel particles

The procedure for the synthesis of the PVCL-α-CD-Au microgel particles is introduced as the follows. In the first step, an aqueous $HAuCl_4$ solution (0.2 ml, 0.01 M) was added to 4.8 ml PVCL-α-CD solution (2.12 mg ml^{-1}) under vigorous stirring for 30 min. After that, 0.02 ml NaOH solution (1.0 M) was added to the above mixture for the reduction of $HAuCl_4$ in the presence of PVCL-α-CD microgels. The color of the solution changed slowly from light yellow to wine-red. The reaction lasted for 72 hours under magnetic stirring at room temperature. After the reaction, the products were cleaned by dialysis.

Synthesis of Au nanoparticles

Au nanoparticles with radius around 5 nm were prepared according to the seeds growing method.[39] The seeds solution was prepared by adding 0.6 ml of ice-cold, freshly prepared 0.1 M $NaBH_4$ solution into a 20 ml aqueous solution containing 2.5×10^{-4} M $HAuCl_4$ and 2.5×10^{-4} M trisodium citrate solution and stirring for 4 hours at room temperature. Then 7.5 ml of growth solution (containing 2.5×10^{-4} M $HAuCl_4$ and 0.08 M solid cetyltrimethylammonium bromide) was mixed with 0.05 ml of freshly prepared 0.1 M ascorbic acid solution. Afterwards, 2.5 ml of seed solution was added while stirring. The stirring continued for 10 min after the solution turned into wine red. The Au nanoparticles were washed by centrifugation twice before the catalytic reaction.

Catalytic reduction of 4-nitropenol and 2,6-dimethyl-4-nitrophenol

The catalytic activity was investigated as follows. Sodium borohydride solution (0.5 ml, 0.1 M) was added to a Nip solution

(4.5 ml, 0.11 mM) contained in a glass vessel. The solution was purged with N_2 to get rid of oxygen from the solution. Then a given amount of PVCL-α-CD-Au particles was added. Immediately after adding the composite particles, UV-vis spectra of the reaction were taken every 20 s in the range of 250–550 nm. The catalytic process for DMNip is conducted in the same way as that of 4-nitropenol as mentioned above.

Characterizations

The hydrodynamic radius of the samples as a function of temperature was conducted by Zetasizer (Malvern Zetasizer Nano ZS ZEN 3500). FTIR-measurements were carried out at a FT-IR Nexus (Thermo Nicolet). For quantitative measurements about 1 mg of sample was weighed, mixed with KBr and pressed to a pellet. The C–O–C-absorption at 1034 cm^{-1} band was used for integration and to calculate the CD amount according to a calibration line. Colloidal stability was analyzed using a LUMiSizer® from L.U.M. GmbH. The samples were measured at 4000 rpm over 300 cycles each 30 seconds to determine the sedimentation velocity. The UV-vis spectra were measured by Lambda 650 spectrometer supplied by Perkin-Elmer or Agilent 8453. Transmission electron microscope (TEM) images were done with JEOL JEM-2100 at 200 kV. XRD measurements were performed in a Bruker D8 diffractometer in the locked coupled mode (scanning angle from 10° to 90°) with Cu Kα radiation, the incident wavelength is 1.5406 Å. For the accomplished measurements the acceleration voltage is set to 40 kV and the filament current to 40 mA. The amount of Au in the PVCL-α-CD microgels was determined by TGA using a Netsch STA 409PC LUXX. Fifteen milligrams of dried sample was heated to 800 °C under a constant argon flow (30 ml min^{-1}) with a heating rate of 10 K min^{-1}. For the calculation of the surface area (S) of the Au nanoparticles, the density of Au (19.3 g cm^{-3}) was used. TGA and TEM results have been used to obtain the amount and size of Au particles assuming spherical shape of the Au nanoparticles. The size distribution of Au nanoparticles was measured using Image J software based on their TEM images. At least 100 units were counted.

Results and discussion

In situ generation of Au nanoparticles in the PVCL-α-CD microgels

PVCL microgels functionalized with α-CD units[36] have been used as an "active" nanoreactor for the *in situ* generation of Au nanoparticles by direct reduction of $HAuCl_4$ in an alkaline aqueous solution. Two samples with different α-CD contents were prepared. The amount of α-CD in microgels was determined to be 1.03 and 13.08 wt%, respectively (see Fig. S1†). The synthesized polymer particles showed a decrease in size for higher contents, while also the swelling ratio decreased (see Fig. S2 and S3†). As shown in Fig. 1a, monodisperse Au nanoparticles with an average diameter of 5–6 nm have been prepared *via* the reduction of $HAuCl_4$ by PVCL-α-CD microgels without adding any additional reducing agent. The obtained Au nanoparticles, which are uniform in size and shape, are homogeneously immobilized in the microgel carriers. The formation of the Au nanoparticles can be followed by the change in color from light yellow to wine-red of the solution. As shown in Fig. S4 in the ESI,† the presence of a clear plasmon peak at around 530 nm further confirms the formation of Au nanoparticles in the presence of α-CD modified PVCL microgels.[39] In a control experiment, no reduction of Au has taken place in the reaction solution in the absence of microgel particles. The color of the $HAuCl_4$ and NaOH mixture was kept light yellow and no obvious absorbance can be found in the UV-vis spectra (ESI, Fig. S4†). In addition, PVCL microgels without α-CD modification have been also used to produce Au nanoparticles. The molecular structure of PVCL is similar with poly(vinylpyrrolidone), of which the amide group can transform to enol structure with a hydroxyl group under high pH conditions.[40] Like long-chain alcohols, this kind of polymer can work as the reducing agent for the synthesis of metal nanoparticles as well.[41,42] As shown in the TEM image in Fig. 1b, Au nanoparticles are generated in the presence of PVCL microgel particles. However, in this case Au nanoparticles were hard to be immobilized inside the microgels, which are weakly attached to the microgel surface or remain as secondary particles in solution. On the contrary, in the PVCL-α-CD-Au composite particles all of the Au nanoparticles are homogeneously distributed within the α-CD modified PVCL microgels. We believe that this is due to the reason that α-CD can provide an efficient capping on the surface of Au nanoparticles due to the Au–COO^- interaction.[34,51] In the absence of α-CD, the interaction between the formed Au nanoparticles and PVCL networks is not strong enough to keep the Au nanoparticles immobilized inside the microgels. Owing to the hydroxyl groups in the molecular structure of the cyclodextrins, the CDs have been reported as the reducing and

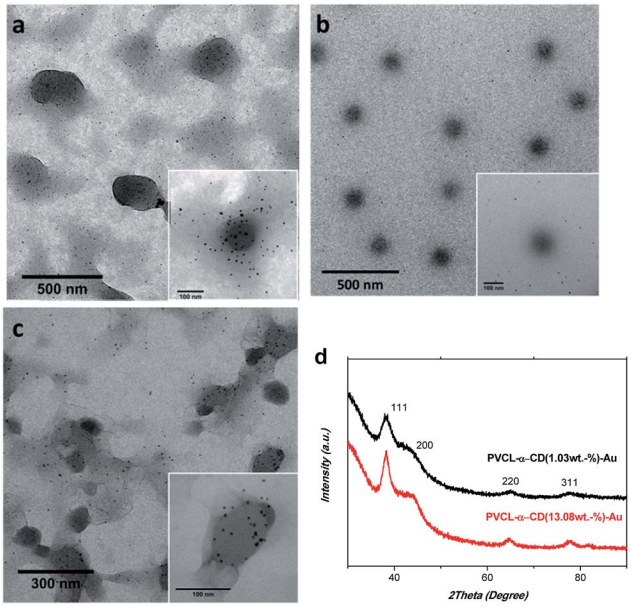

Fig. 1 TEM images of (a) PVCL-α-CD(13.08 wt%)-Au microgel nanoparticles, (b) PVCL-Au microgel nanoparticles and (c) PVCL-α-CD(1.03 wt%)-Au microgel nanoparticles. (d) XRD patterns of PVCL-α-CD(1.03 wt%)-Au (black) and PVCL-α-CD(13.08 wt%)-Au (red).

capping reagent in the synthesis of Au nanoparticles.[33] Interactions of the hydroxyl groups of α-CD with the Au–COO^- surface were monitored by FTIR measurements on a Si crystal. KBr pellets were avoided to minimize the water content of the sample. A shift of 9 cm^{-1} to lower wavenumbers of the OH-absorption band for Au-loaded microgels is observed (ESI, Fig. S5†), which accords with the literature reports.[34,51] In our study, we have demonstrated for the first time that the thermosensitive PVCL microgels modified with α-CD molecules can act efficiently as reducing agent and capping agent for the synthesis of metal nanoparticles.

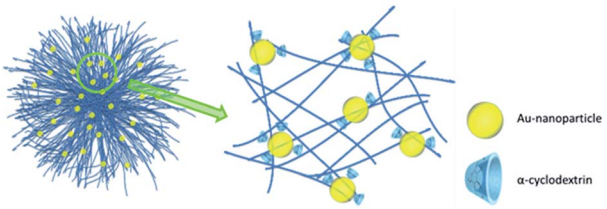

Fig. 2 Schematic overview of the immobilization of Au-nanoparticles in α-CD modified PVCL microgel.

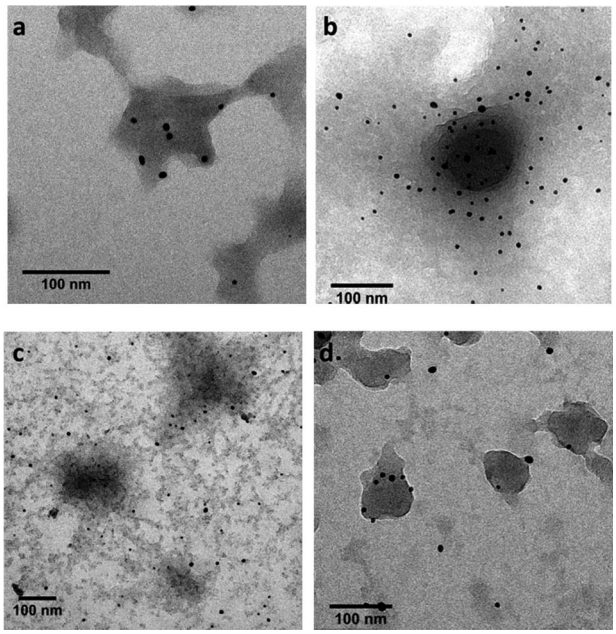

Fig. 3 TEM images of the PVCL-CD-Au microgel particles synthesized with different amount of 0.01 M $HAuCl_4$: (a) 0.1 ml, (b) 0.2 ml, (c) 0.3 ml and (d) 0.4 ml.

The effect of α-CD amount incorporated in the PVCL microgels on the formation of Au nanoparticles has been also studied. Comparing the TEM images shown in Fig. 1a and c, it can be seen that no obvious change in shape and morphology of Au nanoparticles has been found by decreasing the α-CD concentration from 13.08 wt% to 1.03 wt%. Au nanoparticles with diameter of 5.5 ± 0.3 nm have been generated in the PVCL-α-CD(1.03 wt%) microgel particles. Almost all of the Au nanoparticles are immobilized within the microgels. Only the amount of Au nanoparticles generated in the microgel is decreased from 20.07 wt% to 13.26 wt% when decreasing the concentration of α-CD from 13.08 wt% to 1.03 wt%. Because both of the hybrid microgels were synthesized under the same conditions except the amount of α-CD inside the PVCL microgels, this non-linear decrease of Au content against α-CD amount can be explained by the lack of Au precursor leaving free α-CD units that did not bind to Au nanoparticles.

The XRD patterns of these two PVCL-α-CD-Au samples are presented in Fig. 1d. The peaks at $2\theta = 38.34°$, 44.22°, 64.88° and 77.76° correspond to (111), (200), (220) and (311) Bragg reflections of Au, which indicates the face-centered cubic (fcc) structure of the synthesized Au nanoparticles. An estimation of mean size of Au nanoparticles was performed from the full width at half maximum of the (111) Bragg reflection using the Debye–Scherrer equation.[43] The size thus estimated was 4.7 nm for PVCL-α-CD(13.08 wt%)-Au and 4.2 nm for PVCL-α-CD(1.03 wt%)-Au, respectively, which agrees well with the particle size determined from TEM images. Both TEM images and XRD patterns demonstrate that the Au nanoparticles reduced by PVCL microgels with different amount of α-CDs contain almost the same size and crystal structure.

Because of the chemisorption between α-CD and Au nanoparticles (see Fig. 2), the agglomeration of Au nanoparticles can be effectively prevented. As shown in Fig. 3 and Table 1, keeping the amount of α-CDs incorporated in the microgels constant, increasing of the amount of $HAuCl_4$ from 0.1 ml to 0.4 ml leads to an increase in the Au nanoparticle size from 6 nm to 9 nm (the size distribution was shown in Fig. S7†). The UV-vis spectra of the PVCL-α-CD-Au nanoparticles prepared at different $HAuCl_4$ concentrations are presented in Fig. S8 in the ESI.†

It is found that the Surface Plasmon Resonance (SPR) band of these Au nanoparticles red-shifted from 529 nm to 532 nm with band broadening with the increase of the $HAuCl_4$ concentration. In addition, there is a continuous increase of the absorption intensity of the absorption band, which is in good agreement with the finding that the particle size was increased

Table 1 Synthesis of PVCL-CD-Au hybrid particles with different concentration of $HAuCl_4$ in the presence of PVCL-α-CD(13.08 wt%) microgels (solid content 1.06 wt%)

	$HAuCl_4$ (0.01 M)	NaOH (1.0 M)	PVCL-α-CD	d_{Au} (nm) (from TEM)	Au loading (wt%) (from TGA)[a]
1	0.1 ml	0.01 ml	1 ml	6.0 ± 0.3	16.98
2	0.2 ml	0.02 ml	1 ml	5.9 ± 0.3	20.07
3	0.3 ml	0.03 ml	1 ml	7.7 ± 0.8	19.85
4	0.4 ml	0.04 ml	1 ml	9.4 ± 2.2	21.52

[a] A blank TGA experiment was shown in Fig. S6.

with increasing $HAuCl_4$ concentration. When 0.4 ml of $HAuCl_4$ is used, some secondary Au nanoparticles have been found in the system as shown in Fig. 3d.

Temperature-responsive properties and stability of microgel composites

As reported in our previous work, PVCL-α-CD microgels exhibit temperature-responsive properties (see in Fig. S2 and 3 in the ESI†).[36] With the increasing amount of α-CDs modified inside the microgels, a more obvious reduction in the response of the microgels to temperature changes has been observed. Fig. 4 shows the hydrodynamic radii of the microgel particles before and after Au loading as a function of temperature.

The Au-loaded microgel particles show similar volume phase transition temperature (VPTT) behavior as that of the PVCL networks. This result indicates that the immobilization of Au nanoparticles doesn't influence the swelling–deswelling properties of PVCL-α-CDs microgels and proves additionally good distribution of Au in the microgels. Moreover, a much sharper volume transition at 27.5 °C can be observed for the PVCL-α-CD-Au particles. This may be caused by the chemisorption between Au nanoparticles and α-CD molecules in the microgels, which effectively decreases the possible amount of α-CDs as cross-linking units.

The colloidal stability of the Au-loaded sample was compared with its unloaded pure reference sample at 20 °C. As a measure for the colloidal stability we determined the sedimentation velocity of both particle dispersions without and with Au nanoparticles (Fig. S9 and S10†). The samples showed a good colloidal stability in general as they did not sediment completely and showed a relative low sedimentation velocity. Only a small decrease in colloidal stability was observed after Au-loading of the microgel. For a PVCL sample containing 1.03 wt% α-CD, the sedimentation velocity increased from 0.0466 μm s^{-1} for unloaded microgels to 0.0522 μm s^{-1} for particles loaded with Au. For a sample containing 13.08 wt% α-CD, the sedimentation velocity increased from 0.0623 μm s^{-1} to 0.1147 μm s^{-1}. This shows that the microgel dispersion does not lose its stability after deposition of Au nanoparticles, which is important for its use as catalyst system.

Catalytic activity of hybrid microgels

The catalytic reduction of Nip by borohydride has been chosen as the model reaction to test the catalytic activity of the PVCL-α-CD-Au nanoparticles.[44] The reduction of Nip is one of the most often used reactions. It can be easily monitored by UV-vis spectroscopy accurately. More importantly, nitrophenol has been proved to have complexation with cyclodextrin in aqueous solution.[29] Such guest–host complex leads to the shift of the peak of Nip in the UV-vis spectra due to the transfer of the chromophore of the Nip from a polar aqueous environment to a less polar environment within the α-CD cavity.[35,45]

In our study, UV-vis spectra have been taken by mixing Nip solution with α-CD modified PVCL microgel particles. As shown in Fig. 5, the characteristic peak of Nip shifted from 317 nm to 321 nm when PVCL microgel was modified with 13.08 wt% α-CD, while no shift can be determined for the Nip solution mixed with pure PVCL microgels as shown in Fig. S11.† Similar shift can be also found for the PVCL-α-CD(13.08 wt%) microgels after the immobilization of Au nanoparticles. Moreover, when the amount of α-CDs in the PVCL microgels is too less, the shift of the characteristic peak disappears as shown in Fig. S12 in the ESI† for the PVCL-α-CD(1.03 wt%) microgels. According to the literature,[35] such complexation also exists under alkaline conditions that the reduction of Nip starts with. In our experiment, when the pH of the solution was set to 10, similar red-shift of approximate 3 nm was found in the UV-vis spectra when PVCL was modified with α-CD(13.08 wt%) mixing with Nip as shown in Fig. S13.†

The kinetics of Nip reduction in the presence of metal nanocomposite particles can be easily followed by UV-vis spectroscopy.[44] As shown in Fig. 6a, after the addition of PVCL-α-CD(13.08 wt%)-Au nanocomposites, the peak at 400 nm, which

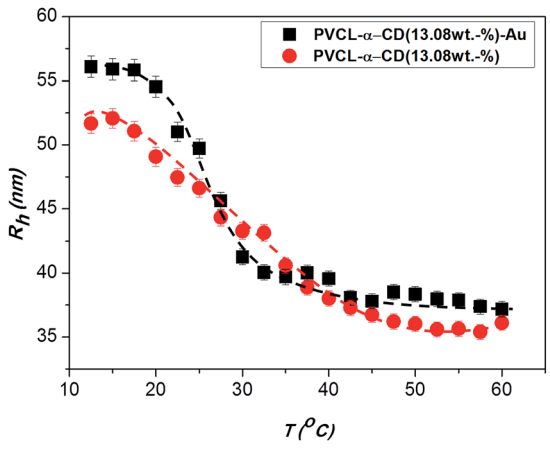

Fig. 4 Hydrodynamic radius of PVCL-α-CD(13.08 wt%) microgels with and without Au nanoparticles as a function of temperature in aqueous solution.

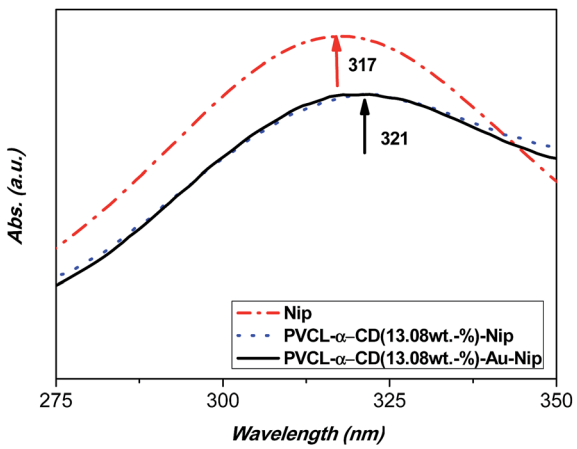

Fig. 5 UV-vis spectra of Nip mixed with PVCL-α-CD(13.08 wt%)-Au microgels (solid line); PVCL-α-CD(13.08 wt%) microgels (dot line) and pure Nip (dash dot line). Concentrations: Nip: 10^{-5} mol L^{-1}; microgels: 0.203 mg ml^{-1}.

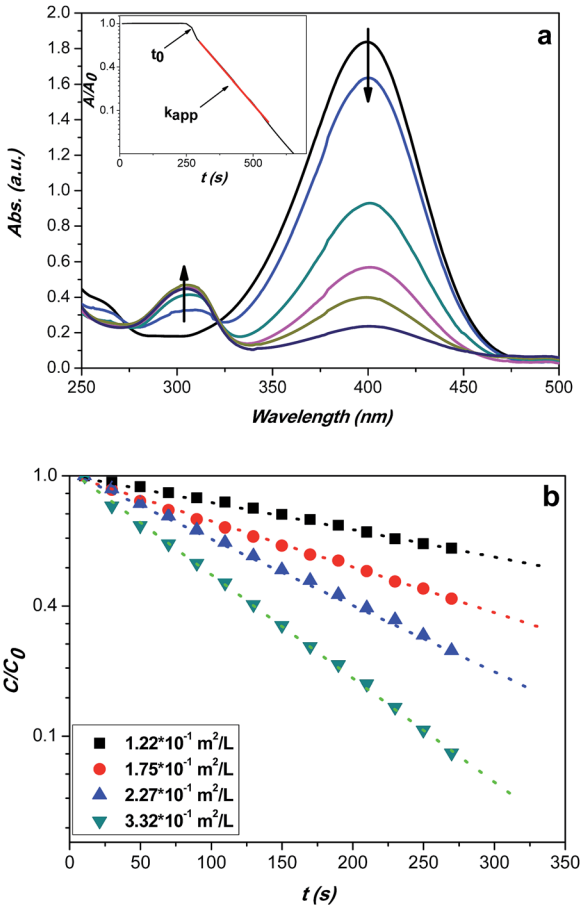

Fig. 6 (a) UV-vis absorption spectra of Nip reduced by sodium borohydride using PVCL-α-CD(13.08 wt%)-Au particles as catalyst at room temperature. The inset shows typical time dependence of the absorption of 4-nitrophenolate ions at 400 nm. (b) Kinetic analysis of the Nip reduced by different amount of PVCL-α-CD(13.08 wt%)-Au hybrid microgel particles at room temperature. (Induction period of the reaction has been subtracted).

is due to the 4-nitrophenate ions, decreases gradually with time and a new peak appears at 290 nm, which results from the product 4-aminophenol. Because of an excess of BH_4^- the reaction follows a pseudo-first order reaction.[46,47] The ratio of the concentration c of the Nip at time t to its original concentration c_0 can be directly given by the ratio of the respective absorbance A/A_0.[48] As shown in Fig. 6b, linear relations between $\ln(c/c_0)$ *versus* time have been obtained in the presence of different amount of PVCL-α-CD(13.08 wt%)-Au catalyst. The apparent rate constant k_{app} is taken from the slope of these linear sections.

Since the catalysis takes place on the surface of the nanoparticles, the catalytic activity depends on the total surface area S of the Au nanoparticles immobilized per unit volume of the PVCL-α-CD microgels. Thus, a kinetic constant k_1 can be defined through normalization to the total surface of the nanoparticles in the system:

$$\frac{dc_{Nip}}{dt} = -k_{app}c_{Nip} = -k_1 S c_{Nip} \quad (1)$$

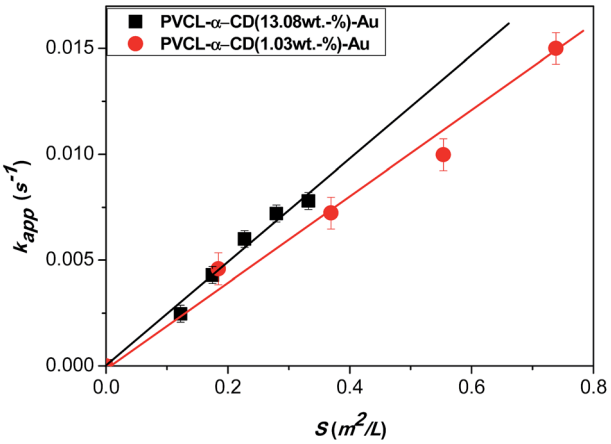

Fig. 7 Rate constant (k_{app}) as a function of surface area S of Au nanoparticles normalized to the unit volume of the system: PVCL-α-CD(13.08 wt%)-Au (solid squares) and PVCL-α-CD(1.03 wt%)-Au (solid circles) at room temperature.

where c_{Nip} is the concentration of Nip and S is the total surface area of the Au nanoparticles in the reaction mixture, respectively.[48] Here the normalized rate constants k_1 have been used for direct comparison in order to exclude the influence of particle size. As shown in Fig. 7, k_1 of 0.025 Ls^{-1} m^{-2} has been determined for the PVCL-α-CD(13.08 wt%)-Au particles, which is slightly larger than that of PVCL-α-CD(1.03 wt%)-Au (k_1 = 0.020 Ls^{-1} m^{-2}).

Since the size and crystal structure of the Au nanoparticles in these two microgels are identical, the difference of the reaction constants for these two samples may be due to the reason that the amount of the α-CDs grafted in the PVCL microgels is different. As shown schematically in Fig. 8, the complexation of Nip with α-CDs that are attached on the Au particle surface favors the adsorption of Nip to the surface of Au nanoparticles. This will increase the local concentration of Nip on the Au nanoparticles surface, which leads to the increase of the catalytic rate constant. This effect will be more obvious when more α-CDs are incorporated into the PVCL microgels. So the PVCL-α-CD(13.08 wt%)-Au particles show higher catalytic activity compared to PVCL-α-CD(1.03 wt%)-Au particles. Meanwhile, according to the literature, the complexation between α-CD and the reduction product 4-aminophenol (Amp) is not so stable as the Nip.[49] As shown in Fig. S14,† no shift of the characteristic peak can be observed for the 4-aminophenol solution mixed with the PVCL-α-CD(13.08 wt%) microgels, which means that it is hard for the α-CDs to form host–guest complex with 4-aminophenol. This indicates that the product cannot influence the reaction speed.

In order to further prove that the CD modified microgels contain certain catalytic selectivity for the target compounds, the catalytic reduction of 2,6-dimethyl-4-nitrophenol (DMNip) by sodium borohydride in the presence of PVCL-α-CD(13.08 wt%)-Au microgels has been studied. DMNip has the similar structure with Nip but greater steric hindrance, which weakens the ability of α-CDs to form host–guest complex with DMNip molecules.[50]

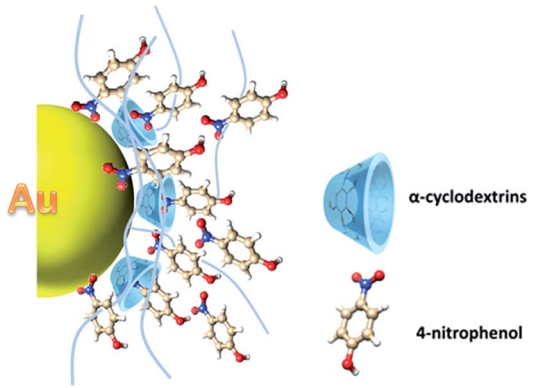

Fig. 8 Immobilization of Nip on the α-CD-modified Au nanoparticle surface.

This has been confirmed from the UV-vis spectra that no obvious shift for the characteristic peak of DMNip has been observed when it is mixed with PVCL-α-CD(13.08 wt%) microgels as shown in Fig. S15 in the ESI.†

The reduction of DMNip by $NaBH_4$ has been monitored by UV-vis spectroscopy that the characteristic absorption peak of DMNip at 431 nm weakens with reaction time and the absorption peak of 2,6-dimethyl-4-aminophenol (DMAmp) at 293 nm increases gradually, which indicates the reduction of DMNip to DMAmp as shown in Fig. S16 in the ESI.†[52] As shown in Fig. 9, a linear relation between k_{app} and the surface S of the Au nanocatalysts can be observed for the reduction of Nip and DMNip. The reaction constants k_1 of different catalysts for both catalytic reactions have been summarized in Table 2 and can be compared with each other directly. First of all, the Au nanoparticles immobilized in the PVCL-α-CD microgels show much higher catalytic activity than that of other catalyst systems for both catalytic reactions. This demonstrates that PVCL-α-CD microgels can work efficiently as reducing and capping agents for the generation of Au nanoparticles with high catalytic activity. More interestingly, it is clearly to see that the rate constant for the reduction of DMNip ($k_1 = 0.018$ Ls^{-1} m^{-2}) is slower than that of Nip ($k_1 = 0.025$ Ls^{-1} m^{-2}) when PVCL-α-CD(13.08 wt%)-Au is used as catalyst. This is opposite to the result of the CTAB-stabilized Au nanoparticles, which do not have complexation with Nip as shown in Fig. S18 in the ESI.† In that case, the catalytic reduction of Nip ($k_1 = 0.008$ Ls^{-1} m^{-2}) is slower than that of DMNip ($k_1 = 0.014$ Ls^{-1} m^{-2}). Similar result also has been reported by K. S. Suslick that the reaction rate of Nip is slower than that of DMNip when using Au nanoparticles encapsulated in porous carbon as catalyst.[52]

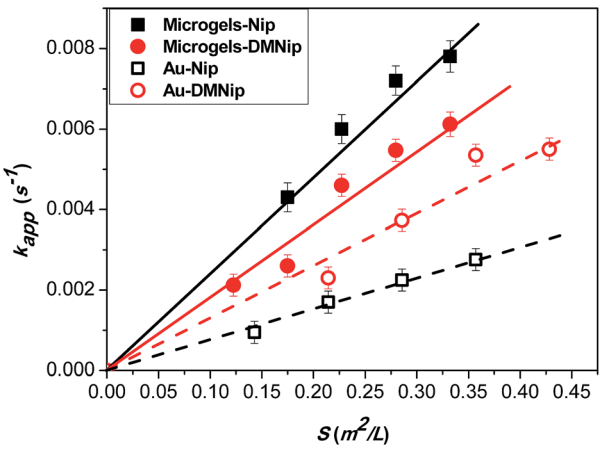

Fig. 9 Rate constant k_{app} of the PVCL-α-CD(13.08 wt%)-Au and pure Au nanoparticles for the catalytic reduction of 4-nitrophenol (Nip) and 2,6-dimethyl-4-nitrophenol (DMNip) by sodium borohydride as a function of surface area S of Au nanoparticles normalized to the unit volume of the system.

The enhancement in the catalytic reduction of Nip in the presence of PVCL-α-CD(13.08 wt%)-Au nanoparticles is due to the complexation of Nip with α-CDs, which increases the local concentration of Nip on the Au nanoparticle surface. In the case of DMNip, this complex interaction is much weaker. That's why the reaction rate is slower compared to that of Nip. This indicates that dependent on the complexability of the compounds with the α-CDs, the incorporation of α-CDs into the microgels will provide Au nanoparticles with specific binding abilities to certain compounds leading to enhanced catalytic activity.

Conclusions

Au nanoparticles have been synthesized *in situ* within the α-CD modified PVCL microgels without adding any reducing agents and surfactants. The size and loading degree of the Au nanoparticles can be controlled by the $HAuCl_4$ amount. The presence of α-CD in the microgels allows homogeneous distribution of Au nanoparticles in colloidal polymer networks. In addition, the immobilization of Au nanoparticles doesn't influence the swelling–deswelling properties of the PVCL-α-CD microgels. Similar VPTT behavior of the PVCL networks has been observed for the PVCL-α-CD-Au hybrid particles. After deposition of Au-nanoparticles inside the microgels, the hybrid particles still

Table 2 Rate constant k_1 of different catalysts for the reduction of 4-nitrophenol (Nip) and 2,6-dimethyl-4-nitrophenol (DMNip)

Sample	Reduction of Nip k_1 (Ls^{-1} m^{-2})	Reduction of DMNip k_1 (Ls^{-1} m^{-2})	d_{Au} (nm) (from TEM)
PVCL-α-CD(13.08 wt%)-Au	0.025	0.018	5.9 ± 0.3
PVCL-α-CD(1.03 wt%)-Au	0.020	—	5.5 ± 0.3
CTAB-stabilized Au	0.008	0.014	10.9 ± 0.4[a]
USP Au/C[b]	2.76×10^{-4}	3.31×10^{-4}	31

[a] TEM images of Au nanoparticles have been shown in Fig. S17. [b] USP: ultrasonic spray pyrolysis; calculated according to the data from the ref. 52.

preserve good colloidal stability. The PVCL-α-CD-Au composite particles can work efficiently as catalyst for the reduction of aromatic nitro-compounds. Most importantly, due to the ability of α-CDs to form complexes with specific compounds, the synthesized hybrid microgels show different catalytic activity for the target compounds during the catalytic reactions. A significant enhancement in the catalytic activity has been observed for the reduction of Nip, while no obvious effect has been found for the reduction of DMNip. Considering the selective binding/complexation properties of CDs with a variety of different guest molecules together with the reducing and stabilizing properties of the PVCL-α-CD microgels, the novel hybrid microgels developed in the present study could create new opportunities for functional nanomaterials with possible applications in catalysis.

Acknowledgements

He Jia gratefully acknowledges financial support of CSC scholarship. DS and AP thank VolkswagenStiftung and Deutsche Forschungsgemeinschaft (DFG SFB 985 "Functional Microgels and Microgel Systems) for financial support.

Notes and references

1 M. A. C. Stuart, W. T. S. Huck, J. Genzer, M. Müller, C. Ober, M. Stamm, G. B. Sukhorukov, I. Szleifer, V. V. Tsukruk, M. Urban, F. Winnik, S. Zauscher, I. Luzinov and S. Minko, *Nat. Mater.*, 2010, **9**, 101.
2 J. Gensel, I. Dewald, J. Erath, E. Betthausen, A. H. E. Müller and A. Fery, *Chem. Sci.*, 2013, **4**, 325.
3 J. Zhang, M. Zhang, K. Tang, F. Verpoort and T. Sun, *Small*, 2014, **10**, 32.
4 B. P. Tripathi, N. C. Dubey, F. Simon and M. Stamm, *RSC Adv.*, 2014, **4**, 34073.
5 Z. Wang, B. Tan, I. Hussain, N. Schaeffer, M. F. Wyatt, M. Brust and A. I. Cooper, *Langmuir*, 2007, **23**, 885.
6 D. Palioura, S. P. Armes, S. H. Anastasiadis and M. Vamvakaki, *Langmuir*, 2007, **23**, 5761.
7 S. Wu, J. Dzubiella, J. Kaiser, M. Drechsler, X. Guo, M. Ballauff and Y. Lu, *Angew. Chem., Int. Ed.*, 2012, **51**, 2229.
8 Y. Zhu, L. Fan, B. Yang and J. Z. Du, *ACS Nano*, 2014, **8**, 5022.
9 M. Antonietti, F. Grohn, J. Hartmann and L. Bronstein, *Angew. Chem., Int. Ed. Engl.*, 1997, **36**, 2080.
10 S. Xu, J. Zhang, C. Paquet, Y. Lin and E. Kumacheva, *Adv. Funct. Mater.*, 2003, **13**, 468.
11 H. B. Zhu, Y. X. Li, R. Q. Qiu, L. Shi, W. T. Wu and S. Q. Zhou, *Biomaterials*, 2012, **33**, 3058.
12 M. Horecha, E. Kaul, A. Horechyy and M. Stamm, *J. Mater. Chem. A*, 2014, **2**, 7431.
13 L. A. Lyon, Z. Meng, N. Singh, C. D. Sorrell and A. S. John, *Chem. Soc. Rev.*, 2009, **38**, 865.
14 J. Ramos, A. Imaz and J. Forcada, *Polym. Chem.*, 2012, **3**, 852.
15 K. C. Clarke and L. A. Lyon, *Langmuir*, 2013, **29**, 12852.
16 S. Nayak, D. Gan, M. J. Serpe and L. A. Lyon, *Small*, 2005, **1**, 416.
17 R. Contreras-Cáceres, S. Abalde-Cela, P. Guardia-Girós, A. Fernández-Barbero, J. Pérez-Juste, R. A. Alvarez-Puebla and L. M. Liz-Marzán, *Langmuir*, 2011, **27**, 4520.
18 J. Pérez-Juste, I. Pastoriza-Santos and L. M. Liz-Marzán, *J. Mater. Chem. A*, 2013, **1**, 20.
19 M. Das, L. Mordoukhovski and E. Kumacheva, *Adv. Mater.*, 2008, **20**, 2371.
20 D. Suzuki, Y. Nagase, T. Kureha and T. Sato, *J. Phys. Chem. B*, 2014, **118**, 2194.
21 Y. Lu, Y. Mei, M. Drechsler and M. Ballauff, *Angew. Chem., Int. Ed.*, 2006, **45**, 813.
22 Y. Lu, S. Proch, M. Schrinner, M. Drechsler, R. Kempe and M. Ballauff, *J. Mater. Chem.*, 2009, **19**, 3955.
23 A. Pich, J. Hain, Y. Lu, V. Boyko, Y. Prots and H. Adler, *Macromolecules*, 2005, **38**, 6610.
24 M. Aslam, L. Fu, M. Su, K. Vijayamohanan and V. P. Dravid, *J. Mater. Chem.*, 2004, **14**, 1795.
25 M. R. Nabid, Y. Bide and M. Niknezhad, *ChemCatChem*, 2014, **6**, 538.
26 K. Kim, K. L. Kim and S. J. Lee, *Chem. Phys. Lett.*, 2005, **403**, 77.
27 B. D. Busbee, S. O. Obare and C. J. Murphy, *Adv. Mater.*, 2003, **15**, 414.
28 S. Mössmer, J. P. Spatz, T. Aberle, J. Schmidt, W. Burchard and M. Möller, *Macromolecules*, 2000, **33**, 4791.
29 T. K. Sau, A. Pal, N. R. Jana, Z. L. Wang and T. Pal, *J. Nanopart. Res.*, 2001, **3**, 257.
30 C. E. Hoppe, M. Lazzari, I. Pardiñas-Blanco and M. A. López-Quintela, *Langmuir*, 2006, **22**, 7027.
31 M. Zhou, B. X. Wang, Z. Rozynek, Z. H. Xie, J. O. Fossum, X. F. Yu and S. Raaen, *Nanotechnology*, 2009, **20**, 505606.
32 G. Agrawal, M. P. Schürings, P. V. Rijn and A. Pich, *J. Mater. Chem. A*, 2013, **1**, 13244.
33 J. Bai, Q. B. Yang, M. Y. Li, S. G. Wang, C. Q. Zhang and Y. X. Li, *Mater. Chem. Phys.*, 2008, **111**, 205.
34 T. Huang, F. Meng and L. M. Qi, *J. Phys. Chem. C*, 2009, **113**, 13636.
35 A. Buvari and L. Barcza, *J. Chem. Soc.*, 1988, **1**, 1.
36 M. J. Kettel, F. Dierkes, K. Schaefer, M. Moeller and A. Pich, *Polymer*, 2011, **52**, 1917.
37 H. Mihaela, P. Marcel, R. Helmut and A. Valentina, *Cellul. Chem. Technol.*, 2005, **39**, 389–413.
38 A. Harada, M. Furue and S. Nozakura, *Macromolecules*, 1976, **9**, 701–704.
39 N. R. Jana, L. Gearheart and C. J. Murphy, *Langmuir*, 2001, **17**, 6782.
40 C. Graf, D. L. J. Vossen and A. Imhof, *Langmuir*, 2003, **19**, 6693.
41 I. Washio, Y. J. Xiong, Y. D. Yin and Y. N. Xia, *Adv. Mater.*, 2006, **18**, 1745.
42 Y. J. Xiong, I. Washio, J. Y. Chen, H. G. Cai, Z. Y. Li and Y. N. Xia, *Langmuir*, 2006, **22**, 8563.
43 H. P. Klug and L. E. Alexander, *X-Ray Diffraction Procedure*, John Wiley & Sons, New York, 1974, p. 656.
44 S. Wunder, F. Polzer, Y. Lu, Y. Mei and M. Ballauff, *J. Phys. Chem. C*, 2010, **114**, 8814.

45 T. Loftsson, *Remington: the science and practice of pharmacy*, Pharmaceutical Press, 2012, ch. 33, p. 687.
46 K. Esumi, R. Isono and T. Yoshimura, *Langmuir*, 2004, **20**, 237.
47 S. K. Ghosh, M. Mandal, S. Kundu, S. Nath and T. Pal, *Appl. Catal., A*, 2004, **268**, 61.
48 P. Hervés, M. Pérez-Lorenzo, L. M. Liz-Marzán, J. Dzubiella, Y. Lu and M. Ballauff, *Chem. Soc. Rev.*, 2012, **41**, 5577.
49 M. V. Rekharsky and Y. Inoue, *Chem. Rev.*, 1998, **98**, 1875.
50 M. Ma and D. Q. Li, *Chem. Mater.*, 1999, **11**, 872.
51 J. Svlvestre, A. V. Kabashin, E. Sacher, M. Meunier and J. H. T. Luong, *J. Am. Chem. Soc.*, 2004, **126**, 7176.
52 J. R. Guo and K. S. Suslick, *Chem. Commun.*, 2012, **48**, 11094.